Published in final edited form as:
Chem Phys. 2018 ; 512: . doi:10.1016/j.chemphys.2018.04.022.

Optical Properties of Meloxicam in the Far-Infrared Spectral Region

Yusuf Samet Aytekin[1], **Mustafa Köktürk**[2], **Adam Zaczek**[3], **Timothy M. Korter**[3], **Edwin J. Heilweil**[4], and **Okan Esenturk**[1,*]

[1]Department of Chemistry, Middle East Technical University, Ankara 06100, Turkey

[2]Nobel Pharmaceuticals Research and Development Center, Düzce 81100, Turkey

[3]Department of Chemistry, Syracuse University, Syracuse, NY 13244-4100, USA

[4]Engineering Physics Division, National Institute of Standards and Technology, Gaithersburg, MD 20899, USA

Abstract

One of the most commonly used nonsteroidal anti-inflammatory active pharmaceutical ingredient called Meloxicam has been characterized spectroscopically both by Terahertz (THz) time domain spectroscopy (THz-TDS) and by Fourier Transform Infrared (FTIR) spectroscopy in far-IR regions of electromagnetic spectrum; 0.2 THz to 20 THz. While many relatively sharp features are observed in the far-IR range between 2 THz to 20 THz as expected for being an organic substance, very distinct and relatively strong absorption bands are also observed at 1.00, 1.66, 2.07 and 2.57 THz in the THz range. These well separated, defined, and fairly strong spectral features can be used for discrimination and quantification of Meloxicam in drug analysis. Frequency dependent refractive index of the drug was determined in a range of 0.2 THz and 2.7 THz, where an almost constant index was observed with an average index of 1.75. Powder XRD, and solid-state Density Functional Theory (SS-DFT) calculations were utilized to determine the crystalline form of the Meloxicam sample in its enolic crystalline form. Single molecule DFT calculations were also performed in all four possible structures of Meloxicam. In addition, the capability of THz waves transmission through common packaging materials is demonstrated for possibility of future on-site analysis. The results suggest that drug analysis will be possible to perform not only at every stage of manufacturing without destruction but also directly at the shelf of a market after development of portable THz technologies.

Keywords

THz-TDS; infrared spectroscopy; active pharmaceutical ingredients (API); API characterization

[*]Corresponding author. Tel.: +90 (312) 2103243; Fax: +90 (312) 2103200, eokan@metu.edu.tr.

1 Introduction

Application of THz waves have been diverse in many areas such as molecular spectroscopy[1], solid state physics[2,3], biology[4–6], imaging[7], and pharmaceuticals[8–11]. This frequency range covers collective vibrational or torsional modes in condensed-phase media, and rotational and vibrational modes of molecules. Thus, it is generally referred to as a spectral fingerprinting region similar to the mid-infrared range. The long wavelengths of THz radiation enables deeper penetration or transmission through many materials like skin, paper, plastic, many synthetics, textiles, etc. Thus, both identification and quantification of an Active Pharmaceutical Ingredients (API) of a drug becomes possible with its molecular fingerprints even if it is covered with the visibly opaque but THz transparent polymeric materials, such as blister packs. In addition, its low energy makes it non-invasive and safe and eliminates the worry of a change in drug morphology or form during the analysis/measurements. With these attractive features THz spectroscopy is recently gaining significant attention in characterization of drugs because of its potential use in identification (including discrimination of polymorphs) and quantification of API. [9,10,12–15]

A recent study by Strachan et al. had shown that different solid-state forms of four different pharmaceutical compounds has very unique terahertz spectra in region of 0.1 THz to 2.25 THz arising from the molecular nature of the chemicals and their crystallinity in each polymorph.[9] In addition, they successfully quantified all four chemicals and two different forms using partial least-squares analysis. In their study Ge et al. presented clear identification of 5 different polymorphs of furosemide using their spectral features between 0.2 THz and 1.6 THz.[8] In a study by Zeitler et al. the sensitivity of THz spectroscopy has been exploited in order to study temperature dependent polymorphism of Carbamazepine in the frequency range between 0.1 THz and 2.85 THz.[16] In a similar study by Sibik et al. crystallization and phase changes of paracetamol was successfully followed by terahertz. [17]

In the pharmaceutical industry, one of the major efforts is to obtain drugs with optimum bioavailability, stability, and solubility besides maximizing its efficacy. Any change in molecular structure (even transitions within the polymorphic forms) prior to, during, or after manufacturing of the drug may result in an unwanted change in solubility, bioavailability, dissolution rate and possibly become a danger to human health[18]. In addition to a change in form of the API, the cocrystals formed during manufacturing could show unique solubility, dissolution rate, hydration stability, and bioavailability.[19,20] It has been shown that cocrystal formation processes could be investigated by using terahertz spectroscopy. [21,22] Therefore, characterization techniques must play a significant role in every part of the manufacturing processes. Common techniques used are X-ray diffractometry, differential scanning calorimetry, IR and Raman spectroscopies and solid state NMR.[23–26] In addition, Spatially Offset Raman spectroscopy (SORS) is a recently developed technique that is applicable on characterization of packaged pharmaceuticals, concealed drugs, and raw pharmaceutical materials non-invasively in their packages and containers.[27,28] Although it is a promising technique, it does have few restrictions. Since the laser employed in SORS is generally in the visible or NIR region the container or the protective cover thickness could

be high enough and may hinder penetration of the laser. In addition, the technique may suffer from fluorescence signals emitted from API, packaging, capsule shell, tablet coating, or plastic container of the drug, and end up with noise suppressing the actual API signal. THz spectroscopy is an emerging and very promising new technique, which does not suffer from fluorescence contamination and has a greater penetration capability with its much longer wavelength. With the aforementioned advantages it is expected that THz methods will take its position as a complementary technique in the pharmaceutical industry in the near future.

The most common market form for pharmaceutical dosage of a drug is formed solid unit doses, commonly known as tablets, sold in blister packs. A tablet mainly contains the drug and inert fillers and binders (excipients) and are being analyzed before, during, and after manufacturing for content, quantity, and homogeneity. Prior to production, form of API and bulk pharmaceutical chemicals (excipients) are checked and confirmed. During the mass production, tablets are also tested for any change in the form of API when necessary. API should be dispersed in a tablet homogenously since controlled release for certain period may be required. Tablets may also be checked for having right amount of coating for controlled release of the drug or to protect for degradation due to harsh acidic conditions of the stomach, etc. In a recent study Lin et al. demonstrated the capability of THz spectroscopy to measure tablet coating thickness.[29] Furthermore, tablets are also analyzed for shelf life prior to marketing under simulated market conditions since an API may have limited stability and may change its form during storage. It would be necessary to characterize finished pharmaceuticals, if possible, right at the shelf on the market for further degradation due to the storage conditions in markets or pharmacies. Thus, THz spectroscopy appears to be a really good candidate to monitor tablets or drugs before, during, and after manufacturing processes for its morphology, homogeneity, and the tablet coating quality.

In this study we present optical properties of a pharmaceutically important drug called Meloxicam over the broad spectral range; 0.2 THz to 20 THz. Meloxicam is an anti-inflammatory drug having analgesic and fever reducing effects and may also be used for arthritis treatment. In addition to absorption spectra and frequency dependent index of the pure Meloxicam, the spectra of the API were collected in PE matrix at various concentrations to simulate the excipients effect on the spectra, by which the capability of THz spectroscopy for quantitative characterization of Meloxicam was also investigated. Moreover, low temperature (77 K) spectra of the API is compared to room temperature spectra. Solid state DFT and single molecule DFT simulations are utilized to confirm/identify the crystal structure and determine the internal and phonon vibrational modes in the low frequency region of the spectrum. The measured spectra of Meloxicam are also a significant contribution to the collection of drug spectra currently being accumulated in the literature. Finally, THz spectra of Meloxicam samples were also collected through actual packaging materials to demonstrate the possibility of non-invasive and non-destructive analysis when the technology becomes readily portable.

2 Experimental

Meloxicam (PubChem CID 54677470, $C_{14}H_{13}N_3O_4S_2$) was obtained from Nobel R&D center in fine powder form and was used without further purification.[*1] The packaging materials were obtained from the package of the commercialized drug named Melox (Nobel Pharma). High density polyethylene (PE) was obtained from Micro Powders Inc. with a particle size of 10 μm. Samples were measured as pellets having 13 mm diameter. The mixture pellets at 5 wt%, 7.5 wt%, and 10 wt% concentrations in PE were prepared under 67 MPa (1 ton per 0.2 in^2) pressure for 20 seconds and the pure pellet were prepared under 67 MPa pressure for 10 minutes with mild vacuum. Since the sample and PE mixes well, no grinding or further processing was needed. No charge or static effect was noticed during mixing. In their study Wu et al. has shown effect of purging time prior to measurement mainly on the high frequency region.[15] We have also observed humidity effect on our pellets thus the sample and the reference pellets were measured at the same purging time (10 min) and flow rate in order to minimize this effect. The Meloxicam structure and its crystalline form in the solid sample was confirmed by ^{1}HNMR and Powder X-ray analysis, respectively. Low temperature (77 K) THz-TDS and THz-FTIR spectra of pure and PE mixture samples were collected with NIST THz-TDS and FTIR spectrometers.

Terahertz Spectroscopy Systems

Two THz time domain spectrometers (METU, TURKEY and NIST, USA), and two commercial FTIR spectrometers (Thermo Nicolet 6700, METU and Thermo Nicolet 550, NIST) were used to cover the spectral absorption range from 0.2 to 20 THz. The METU setup is similar to general TDS systems. The general characteristics of the METU THz-TDS setup and some of the differences are as follows. The light source is a mode-locked Ti:Sapphire oscillator laser (Coherent Mantis, 80 MHz, 80 fs pulsewidth, 800nm central wavelength with ca. 80 nm bandwidth). In the generation arm, the pump beam was focused onto an LT-GaAs photoconductive antenna array (BATOP, iPCA-21–05-1000–800-h), where the excited electrons are accelerated by an applied bias voltage of 15V at 8 kHz. The generated THz beam is guided by off-axis parabolic mirrors (OAPM) in 8F configuration, in which the light is collimated after the generation, focused onto a sample, collected and collimated with other off-axis mirrors, and then focused onto a 500 μm <110> ZnTe crystal (MTI corp.) for THz radiation mapping with 800 nm beam. THz beam pulse-shape is recorded with a combination of quarter waveplate (QWP), Wollaston prism (WP), balance photodiode (BPD), lock in amplifier, and a computer. The spectrometer set-up is shown in Scheme 1. THz pulse-shapes in the time domain and their corresponding frequency domain spectra of a pure meloxicam sample and a reference as an example are given in Figure 1. Details of the 1 KHz amplified NIST THz-TDS setup is given elsewhere.[30]

All THz-TDS measurements were done in a dry air purged environment in order to minimize any water vapor attenuation effects. Humidity was sustained at less than 1% during measurements at all times. The frequency domain spectra were obtained by fast

[*1]Certain commercial equipment or materials are identified in this paper to adequately specify the experimental procedures. In no case does the identification imply recommendation or endorsement by NIST, nor does it imply that the materials or equipment identified are necessarily the best available for the purpose.

Fourier transforms of the time domain data with Hanning window function to extract optical properties of our samples using common software. All FTIR measurements were carried out at an effective working range of 1.5–20 THz. All spectra were collected in the same dry air purged environment. TDS and FTIR spectra presented below were obtained using all four instruments but 77K data was taken using the two NIST apparatus.

Density Functional Theory (DFT) Modelling:

Solid-state density functional theory (DFT) simulations were performed using the CRYSTAL17[31] software package. Structural optimizations were done with fixed lattice parameters based on previously published single crystal X-ray data at room temperature[32]. The atoms were allowed to relax within the fixed lattice parameters with an energy convergence criterion of $\Delta E < 10^{-8}$ Hartree. The Becke, 3-parameter, Lee-Yang-Parr (B3LYP)[33] functional was used with the def2-SVP[34] basis set. To account for weak intermolecular London dispersion forces, all calculations employed Grimme's DFTD3 correction[35,36] which includes a BJ-damping atom-atom term[36]. A total of 112 k points in the irreducible Brillouin zone were found to be sufficient for accurate energy convergence (keyword SHRINK = 6). A large integration grid was used (keyword XXLGRID), corresponding to a pruned (99, 1454) grid. Truncation criteria used to define the Coulomb and Hartree-Fock exchange series (keyword TOLINTEG) were set to 10^{-8}, 10^{-8}, 10^{-8}, 10^{-8}, 10^{-16} Hartree. The resulting structure from the geometry optimization was used for a frequency analysis to determine the frequencies of the vibrational normal modes and infrared intensities via the Berry phase method[37]. Central-difference formula numerical derivatives were used in the frequency calculation (keyword NUMDERIV = 2) and based on two displacements for each atom along each Cartesian direction. For frequency simulations, a stricter $\Delta E < 10^{-10}$ Hartree energy convergence was used.

Single molecule (SM) spectra were obtained by B3LYP/G-631+G(d,p) in Gaussian Revision A.02[38] at TUBITAK ULAKBIM, High Performance and Grid Computing Center (TRUBA). SM calculations were performed for four different structures of the Meloxicam; enolic, zwitter ionic, cationic, and anionic. Starting geometries were optimized prior to the frequency calculations (Figure 2). No negative frequencies were observed in the calculations confirming minimal energy structures.

3 Results and discussion

In this study we present optical properties of one of the most commonly used nonsteroidal anti-inflammatory API called Meloxicam in the frequency range of 0.2 THz to 20 THz. Figure 3a shows the frequency-dependent THz absorption coefficient and refractive index of pure Meloxicam between 0.2 and 2.7 THz. The refractive index was directly obtained from the sample thickness and phase delay information from the FFT analysis. Meloxicam has well separated, prominent absorption bands located at 1.00 THz, 1.66 THz, 2.07 THz (with a shoulder at ca. 2.15), and 2.57 THz at room temperature. The sharp band at 1.00 THz is especially well-resolved in this spectral region where THz-TDS systems in general have the highest signal-to-noise ratio. Observing such well-resolved and strong features are very encouraging since the absorption bands of pharmaceutical drugs in the THz region are

usually very broad and overlap with each other resulting in an almost featureless spectrum. This almost featureless spectral behavior hinders clear drug identifications and quantifications. Therefore, the observed features of Meloxicam are promising characteristic features that can be used for identification and quantification of the drug in a commercial sample when the THz technology advances for portable applications. In addition to spectral features of Meloxicam, the frequency-dependent refractive index was also determined in the same THz range (Figure 3a, top). The index decreases very slightly with frequency and results an average index of 1.75. The observed decrease is so small that it may be considered as constant. The derivative shape occurrences of the refractive index of Meloxicam are well correlated with the strong absorptions observed at those frequencies. The refractive index of Meloxicam is in the expected range of similar drugs.[39]

Meloxicam has four different conformational structures; anionic, cationic, zwitter-ionic and enolic,[14] as shown in Figure 2, leading to different crystalline forms of meloxicam. The structure of the received sample was investigated by H-NMR (see Figure 4(a)). The resonance signals and their ratio confirm the general structure of Meloxicam; however, basic H-NMR spectroscopy is not sensitive enough to determine which one of the four structures exists or is dominant in the sample. Therefore, there is a need for further analysis and help from theoretical investigation to associate the observed bands with the crystalline form of the Meloxicam. The powder XRD diffractogram of the sample is given in Figure 4(b). XRD patterns observed from the sample matches very well with the enolic form reported in the patent.[40] None of the strong diffraction lines associated with the zwitter-ionic at 2Theta angles of ca. 11.8º (strongest) and 15.2º or strong lines of any other form are observed. This suggests that the dominant form is the enolic form in the solid Meloxicam sample; however, we should note that powder XRD might not be sensitive to amounts less than 5 wt%, which is a significant amount that may result in contributions to the collected THz and far-IR spectra. Therefore, single molecule (for all four structures) and solid state (only enolic structure) DFT frequency calculations for Meloxicam were carried out. In addition, low temperature (77 K) THz and far-IR spectra were collected for comparison. Figure 3b presents room temperature (RT, red), and 77K (blue) TDS, solid state (SS-DFT, dotted gray) and single molecule (stick spectrum, orange bars) DFT spectra of the enolic structure. Interestingly, the bands did not sharpen significantly with the decrease in temperature, though 77 K may still be considered reasonably high temperature compare to 4 K, etc. However, we observed a shift toward higher frequency (blue-shift) for every band. The observed blue shift in the vibrational modes suggests a slight change in lattice parameters with decreasing temperature. In addition, an increase in anharmonicity may also have a strong contribution to the observed behavior.[41] The most significant shifts were observed for the 2.07 THz and 2.57 THz bands which have shoulders at RT. Larger shifts of these bands might be due to separation of shoulders from the main band and increase in their peak intensities as the bands are shifted with the decrease in temperature. Figure 3c present the RT and 77 K spectra of the sample in the far-IR region. The band sharpening and collapse of the bandwidth toward the higher frequency side of the band is clear in the figure.

The spectrum obtained with SS DFT calculations of the enolic form of the crystalline structure agree very well with both the THz-TDS and far-IR spectra (Figure 3b and 3d). In addition to Powder XRD data, the strong correlation of the theoretical SS-DFT results to the

experimental spectra confirms that the sample crystal structure is the enolic form. The theoretical calculations predict all the observed normal mode vibrational bands, except the bands at 2.07 THz (and the shoulder at 2.16 THz), which appeared as a combination band in the SS-DFT spectrum at 1.75 THz along with the one at 1.64 THz. Moreover, single molecule DFT spectra for all four structures were also simulated. After frequency scaling, the enolic molecular structure again correlated very well with the experimental spectra (Figure 3b) except for the band at 2.57 THz. Observation of this band both in experimental spectra and the SS DFT calculation but not in the single molecule calculation suggests that the band is a phonon mode, while all the other bands are intramolecular modes. This may also explain the strong splitting of this band with cooling to 77K while all other bands are in the same frequency as the RT experimental ones. The center frequency of the experimental and simulated bands and a description of the observed modes is given in Table 1.

Figure 3(c) presents the far-IR spectra of ca. 5 wt% Meloxicam in PE measured with FTIR spectrometers in a range of 1.5 THz to 20 THz. The spectrum is very rich and has many very strong, well-resolved features in this range. All the resolved features are labelled with their THz frequencies in the figure. The main two features with strong absorptions below 10 THz are located at 3.62 THz and 9.72 THz. With a THz-TDS spectrometer reaching up to 5 THz, the strong 3.62 THz feature (along with other neighboring bands) would be a very good marker band for identification and quantification of Meloxicam. However, it should be noted that most commonly used THz-TDS spectrometers have a THz range between 0.1 THz and 3 THz with the highest S/N at ca. 1 THz.

Figure 5(a) presents the THz spectrum of 5 wt% 7.5 wt%, and 10 wt% Meloxicam in PE samples along with the pure Meloxicam spectra. All the main vibrational features (at 1.00 THz, 1.66 THz, and 2.07 THz) of Meloxicam are observed even for the 5 wt% sample. Such good agreement with the pure Meloxicam spectrum shows that the PE matrix, acting as a simulated excipient, has little or very small effect on the spectral features. The band at 2.57 THz could not be observed possibly due to the loss of bandwidth with the addition of PE and its strong absorption band at 2.23 THz and the higher ones. The spectra of 5 wt% Meloxicam in PE collected with both FTIR (dotted line) and THz-TDS (yellow) are also compared in the Figure 5(a). The bands observed in THz spectrum are also identified in far-IR spectrum at 1.66 THz and ca. 2.01 THz within the common frequency range even though the bands intensities are barely above the noise level in the far-IR spectrum due to much lower S/N in this region. Both techniques appear to be complementary to each other to obtain wide spectral coverage (0.1 THz to 20 THz) to determine the characteristic absorption features of Meloxicam over such a broad range.

The relatively strong and well-resolved bands of Meloxicam in the THz range present an opportunity for quantitative analysis. Therefore, we have investigated the concentration dependence of all three bands (1.00 THz, 1.66 THz, and 2.1 THz) accessible to TDS methods. We expected to have the best linear dependence response from the 1 THz band since the THz-TDS instrument has the best signal-to-noise ratio at around 1 THz (see Figure 1b). A simple baseline correction was done on the spectra of 5 wt%, 7 wt%, and 10 wt% Meloxicam samples to eliminate the effect of variation in scattering by each sample. An example of the baseline corrected spectra is given in the inset of Figure 5(b) for the band at 1

THz. Figure 5(b) presents the plot of peak absorbance versus concentration at all three frequencies with a fitted line crossing zero referring to zero concentration. As expected, the absorbance increases linearly with Meloxicam content in PE and appears to obey the Beer-Lambert Law. A slightly lower absorbance for the 10 wt% sample at all three frequencies compared to the fitted line might be because of either not being able to adequately correct the baseline or because of changes in refractive index at high analyte concentration where the limit of the Beer-Lambert law is reached. In addition, stronger deviation from the fit for the 2.1 THz band absorbance with concentration arises from the very low S/N at these frequencies. The results clearly suggest that the band at 1 THz and 1.66 THz (and possibly 2.1 THz) can be used for quantification of the Meloxicam within excipients and tablets.

Finally, the THz transparency of packaging materials used for disseminating the commercial drug was examined for the feasibility of drug measurements while the drug is in its package. Figure 6(a) demonstrates the time domain THz field pulse-shapes of various parts of the package (plastic blister piece, the folding carton with plastic blister). The packaging materials significantly attenuate the THz transmission for frequencies greater than 1.5 THz (see Figure 6(b)). However, despite all this attenuation there appears to be sufficient THz transmission for API measurements in the tablet. Additionally, the frequency dependent THz absorbance is featureless for both the blister cage and folding carton cover especially around 1 THz (Figure 6(b)). The absorbance spectra of 5 wt%, 7.5 wt% and 10 wt% Meloxicam in PE collected behind two folding carton and two plastic blister cage pieces is presented in Figure 6(b) with good S/N. One of the stronger Meloxicam bands at 1 THz and its concentration dependence is observed. The results clearly indicate that the THz beam has ability to reach the drug tablet by penetrating through the folding carton and plastic blister and exit the other side of the box. However, it should be noted that these measurements were performed with the standard aluminum foil seal (used to protect and hold the drug in its cavity) removed. Aluminum does not transmit THz light and is known to be a good THz reflector. Thus, the aluminum packaging would enable collection of a THz absorption spectrum in reflectance mode. In this arrangement, using the time domain difference between THz pulses reflecting from both the front surface of the drug and from aluminum foil after double transmission through the sample would potentially enable one to collect reference and sample spectra at once in a one-shot analysis scenario.

4 Conclusion

In this study the optical absorption properties of a commonly used nonsteroidal anti-inflammatory drug called Meloxicam were obtained in the THz and far-IR spectral region covering the very wide range from 0.2 THz to 20 THz. Well resolved spectral features at 1.00 THz, 1.66 THz, 2.07 THz, 2.55 THz, 3.06 THz, and 4.47 THz are observed below 5 THz. The refractive index of pure Meloxicam appears to be decreasing very slightly with increasing frequency, resulting in an average index of 1.75. The powder XRD data of the sample matches very well with the enolic form of the crystal structure of Meloxicam. This crystal form is confirmed with strong correlations between calculated solid state DFT spectra of the enolic form and the experimentally collected THz and far-IR spectra. Isolated molecule DFT calculations showed that all the THz bands within the 1 THz to 3 THz range are intramolecular vibrational modes except the band at 2.57 THz. This also explains the

observed substantial change in the 2.57 THz band with temperature while all others slightly sharpened and shifted to higher frequency. The presented relatively strong and well-resolved bands of Meloxicam in the THz range is an addition to the slowly growing literature of API THz spectra. Even though strong attenuation was observed during penetration and transmission of the THz beam through the packaging materials, it is very promising that it may be possible to collect spectra (and identify and quantify Meloxicam with the help of the band at 1 THz) while the drug is contained in its package. This may even be accomplished with intact aluminum foil containment if THz reflectance spectra are collected. These results are a promising addition to the application of non-destructive THz spectroscopic methods to identify and quantify APIs at the shelf after further technical and reduced costs permit advances in widespread application of THz technology.

Acknowledgements

OE gratefully acknowledges access to Dr. Heilweil's Terahertz facilities to jointly perform room and low temperature FTIR and TDS measurements on Meloxicam pellets at NIST. This work was supported by the Middle East Technical University Projects (08–11-KB2014K120600–1, 07–02-2012005) and through NIST Scientific Technical Research Support (STRS)

REFERENCES

[1]. Konek C, Wilkinson J, Esenturk O, Heilweil E, Kemp M, Terahertz spectroscopy of explosives and simulants: RDX, PETN, sugar, and L-tartaric acid, Proc. SPIE 7311 (2009) 73110K–1–73110K–7. doi:10.1117/12.817913.

[2]. Fan F, Li W, Gu WH, Wang XH, Chang SJ, Cross-shaped metal-semiconductor-metal plasmonic crystal for terahertz modulator, Photonics Nanostructures - Fundam. Appl 11 (2013) 48–54. doi:10.1016/j.photonics.2012.08.001.

[3]. Docherty CJ, Johnston MB, Terahertz properties of graphene, J. Infrared, Millimeter, Terahertz Waves 33 (2012) 797–815. doi:10.1007/s10762-012-9913-y.

[4]. Ashworth PC, Pickwell-MacPherson E, Provenzano E, Pinder SE, Purushotham AD, Pepper M, Wallace VP, Terahertz pulsed spectroscopy of freshly excised human breast cancer., Opt. Express 17 (2009) 12444–12454. doi:10.1364/OE.17.012444. [PubMed: 19654646]

[5]. He M, Azad AK, Ye S, Zhang W, Far-infrared signature of animal tissues characterized by terahertz time-domain spectroscopy, Opt. Commun 259 (2006) 389–392. doi:10.1016/j.optcom.2005.08.029.

[6]. Plusquellic DF, Siegrist K, Heilweil EJ, Esenturk O, Applications of terahertz spectroscopy in biosystems, ChemPhysChem. 8 (2007) 2412–2431. [PubMed: 17990257]

[7]. Chan WL, Deibel J, Mittleman DM, Imaging with terahertz radiation, Reports Prog. Phys 70 (2007) 1325–1379. doi:10.1088/0034-4885/70/8/R02.

[8]. Ge M, Liu G, Ma S, Wang W, Polymorphic forms of furosemide characterized by THz time domain spectroscopy, Bull. Korean Chem. Soc 30 (2009) 2265–2268. doi:10.5012/bkcs.2009.30.10.2265.

[9]. Strachan CJ, Taday PF, Newnham D. a., Gordon KC, Zeitler JA, Pepper M, Rades T, Using terahertz pulsed spectroscopy to quantify pharmaceutical polymorphism and crystallinity, J. Pharm. Sci 94 (2005) 837–846. doi:10.1002/jps.20281. [PubMed: 15736195]

[10]. Strachan CJ, Rades T, Newnham D. a., Gordon KC, Pepper M, Taday PF, Using terahertz pulsed spectroscopy to study crystallinity of pharmaceutical materials, Chem. Phys. Lett 390 (2004) 20–24. doi:10.1016/j.cplett.2004.03.117.

[11]. Shibata T, Mori T, Kojima S, Low-frequency vibrational properties of crystalline and glassy indomethacin probed by terahertz time-domain spectroscopy and low-frequency Raman scattering, Spectrochim. Acta - Part A Mol. Biomol. Spectrosc 150 (2015) 207–211. doi:10.1016/j.saa.2015.05.059.

[12]. Taday PF, V Bradley I, Arnone DD, Pepper M, Using terahertz pulse spectroscopy to study the crystalline structure of a drug: A case study of the polymorphs of ranitidine hydrochloride - Taday - 2003 - Journal of Pharmaceutical Sciences - Wiley Online Library, J. Pharm. Sci 92 (2003) 831–838. [PubMed: 12661068]

[13]. King MD, Buchanan WD, Korter TM, Identification and quantification of polymorphism in the pharmaceutical compound diclofenac acid by terahertz spectroscopy and solid-state density functional theory, Anal. Chem 83 (2011) 3786–3792. doi:10.1021/ac2001934. [PubMed: 21480654]

[14]. Snor W, Liedl E, Weiss-Greiler P, Viernstein H, Wolschann P, Density functional calculations on meloxicam–β-cyclodextrin inclusion complexes, Int. J. Pharm 381 (2009) 146–152. doi:10.1016/j.ijpharm.2009.05.012. [PubMed: 19446616]

[15]. Wu H, Heilweil EJ, Hussain AS, Khan MA, Process analytical technology (PAT): Effects of instrumental and compositional variables on terahertz spectral data quality to characterize pharmaceutical materials and tablets, Int. J. Pharm 343 (2007) 148–158. doi:10.1016/j.ijpharm.2007.05.014. [PubMed: 17590292]

[16]. Zeitler JA, Newnham D. a., Taday PF, Strachan CJ, Pepper M, Gordon KC, Rades T, Temperature dependent terahertz pulsed spectroscopy of carbamazepine, Thermochim. Acta 436 (2005) 71–77. doi:10.1016/j.tca.2005.07.006.

[17]. Sibik J, Sargent MJ, Franklin M, Zeitler JA, Crystallization and Phase Changes in Paracetamol from the Amorphous Solid to the Liquid Phase, Mol. Pharm 11 (2014) 1326–1334. doi:10.1021/mp400768m. [PubMed: 24579729]

[18]. Byrn S, Pfeiffer R, Ganey M, Hoiberg C, Poochikian G, Pharmaceutical Solids: A Strategic Approach to Regulatory Considerations, Pharm. Res. An Off. J. Am. Assoc. Pharm. Sci 12 (1995) 945–954. doi:10.1023/A:1016241927429.

[19]. Friscić T, Fábián L, Burley JC, Jones W, Motherwell WDS, Friščić T, Fábián L, Burley JC, Jones W, Motherwell WDS, Exploring cocrystal-cocrystal reactivity via liquid-assisted grinding: The assembling of racemic and dismantling of enantiomeric cocrystals, Chem. Commun (2006) 5009–5011. doi:10.1039/b613073a.

[20]. Friščić T, Jones W, Benefits of cocrystallisation in pharmaceutical materials science: An update, J. Pharm. Pharmacol 62 (2010) 1547–1559. doi:10.1111/j.2042-7158.2010.01133.x. [PubMed: 21039540]

[21]. Du Y, Zhang H, Xue J, Fang H, Zhang Q, Xia Y, Li Y, Hong Z, Raman and terahertz spectroscopical investigation of cocrystal formation process of piracetam and 3hydroxybenzoic acid, Spectrochim. Acta - Part A Mol. Biomol. Spectrosc 139 (2015) 488–494. doi:10.1016/j.saa.2014.11.109.

[22]. Du Y, Xia Y, Zhang H, Hong Z, Using terahertz time-domain spectroscopical technique to monitor cocrystal formation between piracetam and 2,5-dihydroxybenzoic acid, Spectrochim. Acta - Part A Mol. Biomol. Spectrosc 111 (2013) 192–195. doi:10.1016/j.saa.2013.03.081.

[23]. Riekes MK, Pereira RN, Rauber GS, Cuffini SL, de Campos CEM, Silva MAS, Stulzer HK, Polymorphism in nimodipine raw materials: Development and validation of a quantitative method through differential scanning calorimetry, J. Pharm. Biomed. Anal 70 (2012) 188–193. doi:10.1016/j.jpba.2012.06.029. [PubMed: 22795312]

[24]. Yang C, Mitra AK, Low-level determination of polymorph composition in physical mixtures by near-infrared reflectance spectroscopy, J. Pharm. Sci 90 (2001) 360–370. doi:10.1002/1520-6017(200103)90:3<360::AID-JPS11>3.0.CO;2-U. [PubMed: 11170029]

[25]. Seliger J, Žagar V, Apih T, Gregorovič A, Latosińska M, Olejniczak GA, Latosińska JN, Polymorphism and disorder in natural active ingredients. Low and high-temperature phases of anhydrous caffeine: Spectroscopic (1H–14N NMR–NQR/14N NQR) and solid-state computational modelling (DFT/QTAIM/RDS) study, Eur. J. Pharm. Sci 85 (2016) 18–30. doi:10.1016/j.ejps.2016.01.025. [PubMed: 26826282]

[26]. Docoslis A, Huszarik KL, Papageorgiou GZ, Bikiaris D, Stergiou S, Georgarakis E, Characterization of the distribution, polymorphism, and stability of nimodipine in its solid dispersions in polyethylene glycol by micro-Raman spectroscopy and powder X-ray diffraction., AAPS J. 9 (2007) E361–E370. doi:10.1208/aapsj0903043. [PubMed: 18170983]

[27]. Olds WJ, Jaatinen E, Fredericks P, Cletus B, Panayiotou H, Izake EL, Spatially offset Raman spectroscopy (SORS) for the analysis and detection of packaged pharmaceuticals and concealed drugs, Forensic Sci. Int 212 (2011) 69–77. doi:10.1016/j.forsciint.2011.05.016. [PubMed: 21664083]

[28]. Bloomfield M, Andrews D, Loeffen P, Tombling C, York T, Matousek P, Non-invasive identification of incoming raw pharmaceutical materials using Spatially Offset Raman Spectroscopy, J. Pharm. Biomed. Anal 76 (2013) 65–69. doi:10.1016/j.jpba.2012.11.046. [PubMed: 23298907]

[29]. Lin H, May RK, Evans MJ, Zhong S, Gladden LF, Shen Y, Zeitler JA, Impact of Processing Conditions on Inter-tablet Coating Thickness Variations Measured by Terahertz In-Line Sensing, J. Pharm. Sci 104 (2015) 2513–2522. doi:10.1002/jps.24503. [PubMed: 26037660]

[30]. Esenturk O, Evans A, Heilweil EJ, Terahertz spectroscopy of dicyanobenzenes: Anomalous absorption intensities and spectral calculations, Chem. Phys. Lett 442 (2007) 71–77. doi:10.1016/j.cplett.2007.05.067.

[31]. Erba A, Baima J, Bush I, Orlando R, Dovesi R, Large-Scale Condensed Matter DFT Simulations: Performance and Capabilities of the CRYSTAL Code, J. Chem. Theory Comput 13 (2017) 5019–5027. doi:10.1021/acs.jctc.7b00687. [PubMed: 28873313]

[32]. Luger P, Daneck K, Engel W, Trummlitz G, Wagner K, Structure and physicochemical properties of meloxicam, a new NSAID, Eur. J. Pharm. Sci 4 (1996) 175–187. doi:10.1016/0928-0987(95)00046-1.

[33]. Becke AD, A new mixing of Hartree–Fock and local density- functional theories, J. Chem. Phys 98 (1993) 1372–1377. doi:10.1063/1.464304.

[34]. Weigend F, Ahlrichs R, Balanced basis sets of split valence, triple zeta valence and quadruple zeta valence quality for H to Rn: Design and assessment of accuracy, Phys. Chem. Chem. Phys 7 (2005) 3297. doi:10.1039/b508541a. [PubMed: 16240044]

[35]. Grimme S, Antony J, Ehrlich S, Krieg H, A consistent and accurate ab initio parametrization of density functional dispersion correction (DFT-D) for the 94 elements H-Pu, J. Chem. Phys 132 (2010) 154104. doi:10.1063/1.3382344. [PubMed: 20423165]

[36]. Grimme S, Ehrlich S, Goerigk L, Effect of the damping function in dispersion corrected density functional theory, J. Comput. Chem 32 (2011) 1456–1465. doi:10.1002/jcc.21759. [PubMed: 21370243]

[37]. Noel Y, Zicovich-Wilson CM, Civalleri B, D'Arco P, Dovesi R, Polarization properties of ZnO and BeO: An *ab initio* study through the Berry phase and Wannier functions approaches, Phys. Rev. B 65 (2001) 14111. doi:10.1103/PhysRevB.65.014111.

[38]. Frisch GESMJ, Trucks GW, Schlegel HB, Robb BMMA, Cheeseman JR, Scalmani G, Barone V, Petersson HPHGA, Nakatsuji H, Caricato M, Li X, Izmaylov MHAF, Bloino J, Zheng G, Sonnenberg JL, Ehara TNM, Toyota K, Fukuda R, Hasegawa J, Ishida M, Honda JY, Kitao O, Nakai H, Vreven T, Montgomery JA, Peralta EBJE, Ogliaro F, Bearpark M, Heyd JJ, Kudin JNKN, Staroverov VN, Kobayashi R, Raghavachari JTK, Rendell A, Burant JC, Iyengar SS, Cossi JBCM, Rega N, Millam JM, Klene M, Knox JE, Bakken RESV, Adamo C, Jaramillo J, Gomperts R, Yazyev JWOO, Austin AJ, Cammi R, Pomelli C, Martin GAVRL, Morokuma K, Zakrzewski VG, Salvador ADDP, Dannenberg JJ, Dapprich S, Farkas JCO, Foresman JB, Ortiz JV, and Fox DJ, Gaussian 09, Revision A.02, (2009).

[39]. Zeitler JA, Kogermann K, Rantanen J, Rades T, Taday PF, Pepper M, Aaltonen J, Strachan CJ, Drug hydrate systems and dehydration processes studied by terahertz pulsed spectroscopy, Int. J. Pharm 334 (2007) 78–84. doi:10.1016/j.ijpharm.2006.10.027. [PubMed: 17129691]

[40]. Coppi L, Sanmarti M, Clavo M, Crystalline forms of meloxicam and processes for their preparation and interconversion, US20030109701A1, 2003.

[41]. Ruggiero MT, Zeitler JA, Resolving the Origins of Crystalline Anharmonicity Using Terahertz Time-Domain Spectroscopy and *ab Initio* Simulations, J. Phys. Chem. B 120 (2016) 11733–11739. doi:10.1021/acs.jpcb.6b10248. [PubMed: 27766874]

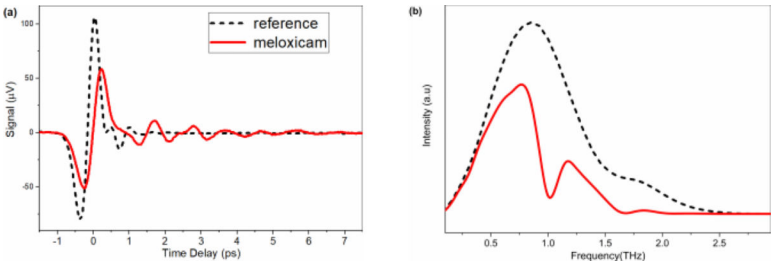

Fig. 1.

(a) THz pulse-shapes in time domain and (b) frequency domain spectra of reference (black) and pure Meloxicam sample (red)

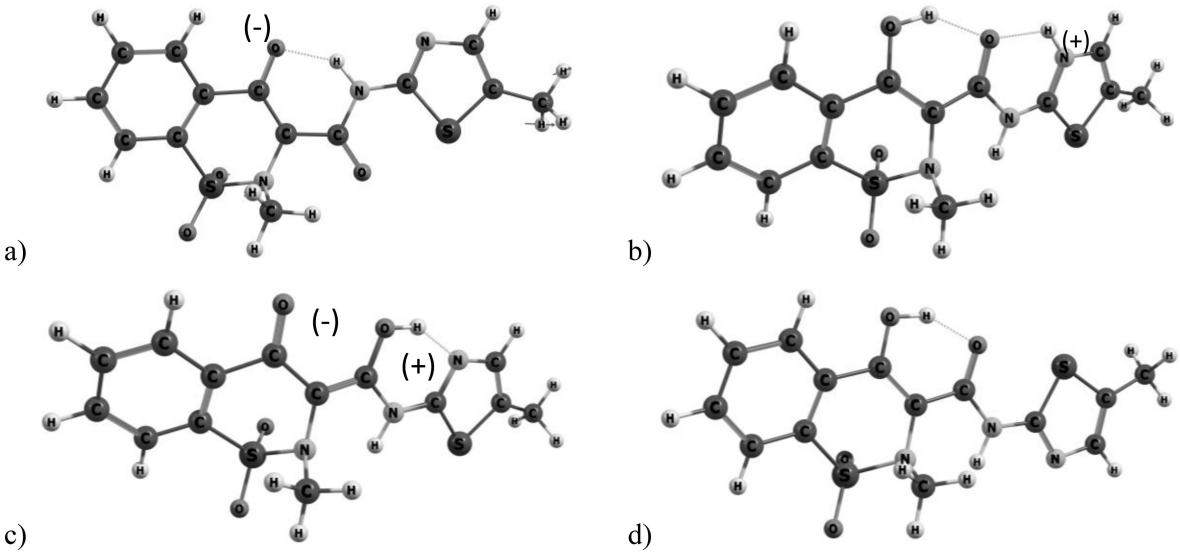

Fig. 2.
Optimized molecular structures of a) anionic, b) cationic, c) zwitter-ionic and d) enolic forms of Meloxicam.

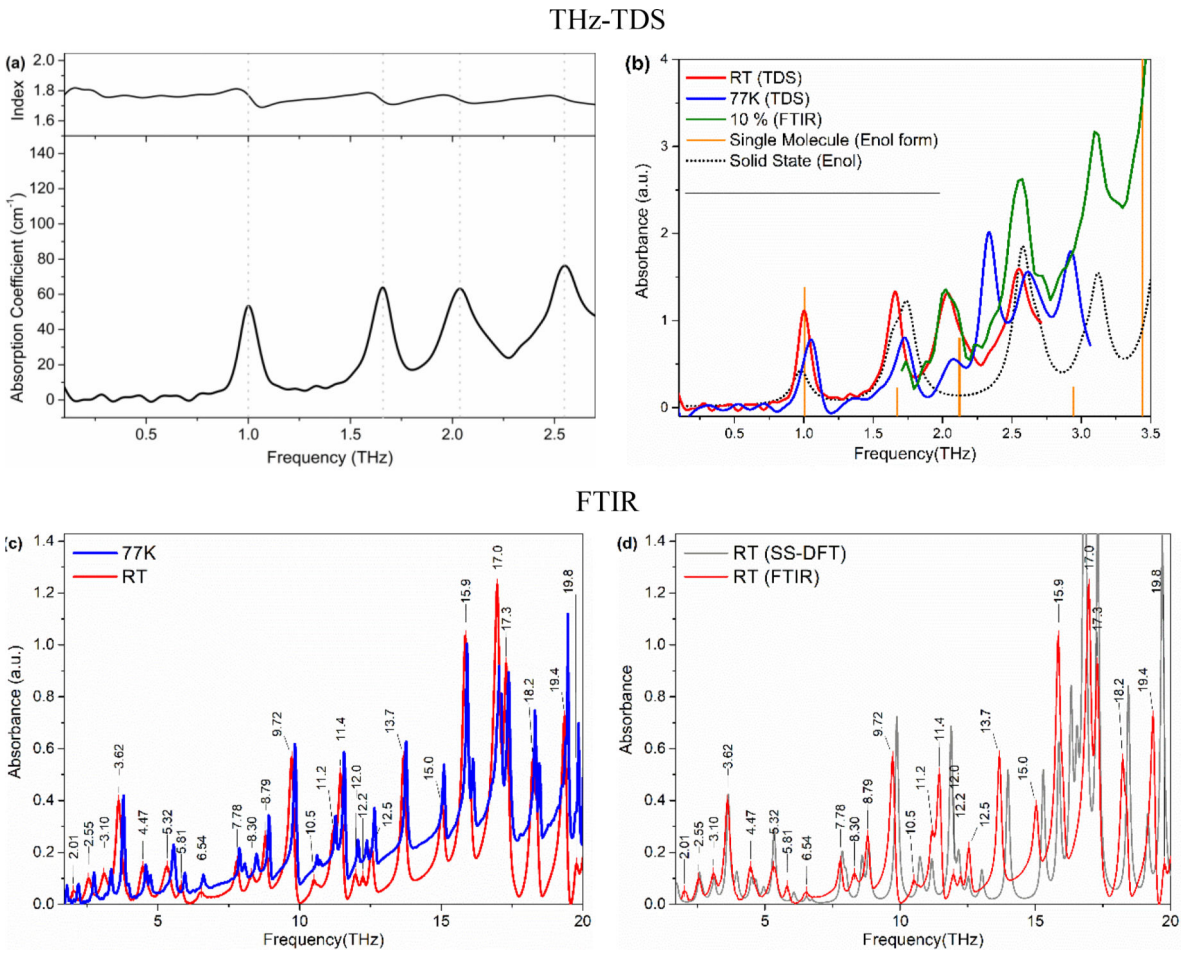

Fig. 3.

(a) Frequency dependent absorption coefficient and refractive index of pure Meloxicam. (b) Solid state (SS, dashed line) and single molecule (SM, orange bars) simulated spectra of enolic Meloxicam in comparison with experimental absorption spectra of Meloxicam sample at room temp (RT, red) and 77 K (blue) and absorption spectra of 10 wt% Meloxicam in PE (FTIR). (c) The far-IR spectra of Meloxicam sample at room temperature (red) and 77 K (blue) over the range of 1.5 THz to 20 THz. (d) Comparison of simulated SS-DFT Meloxicam (enol form) spectrum with RT experimental spectrum of 10% Meloxicam in PE (FTIR). The extremely good spectral match between the SS-DFT spectrum to the experimental one confirms the enolic form of the Meloxicam sample.

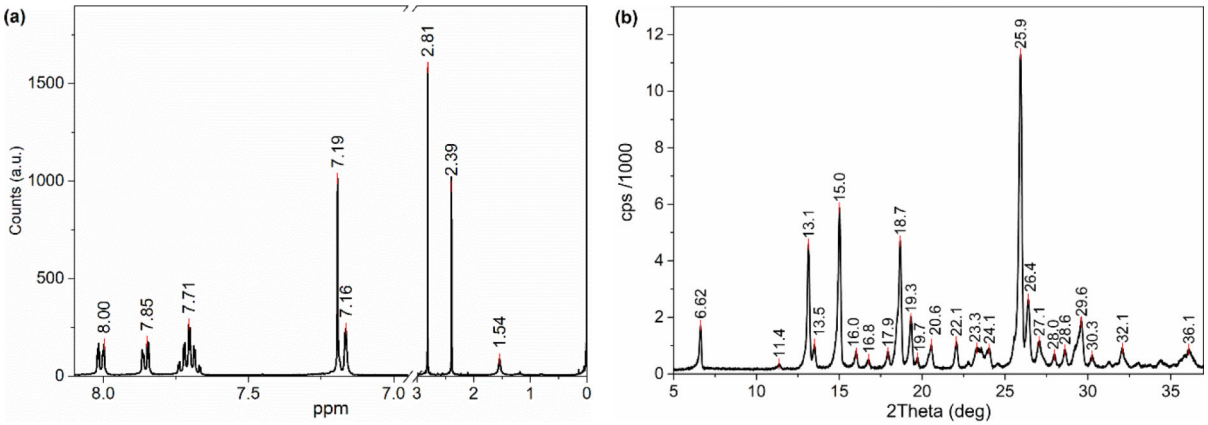

Fig. 4.

a) 400 MHz ^{1}H NMR Spectrum in $CDCl_3$ (there is no signal in the break region between 3 and 6.9 ppm or beyond 8.1 ppm) and b) Powder XRD patterns of the Meloxicam sample.

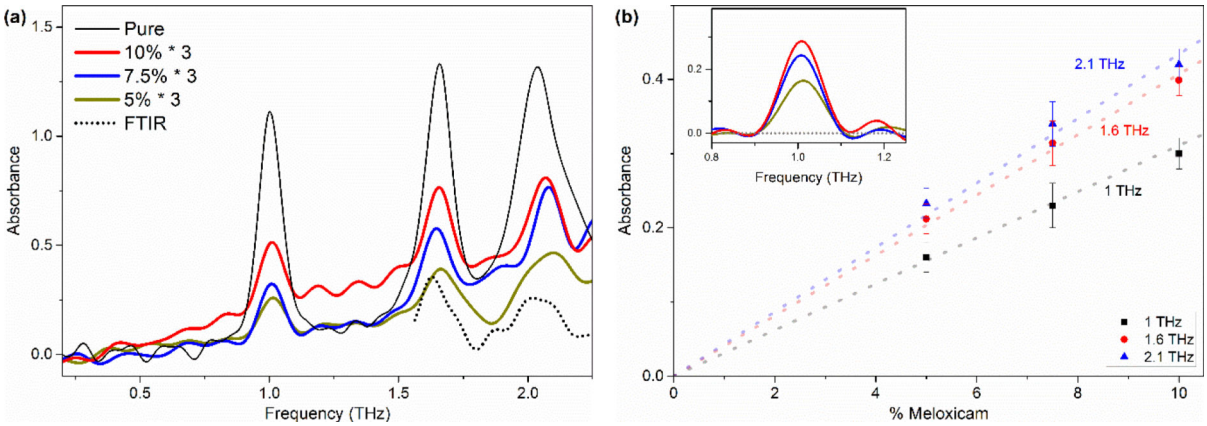

Fig. 5.

(a) THz spectra of pure, 5 %, 7.5 %, and 10 % (w/w) Meloxicam in PE pellets. (b) Concentration vs Absorbance plot of selected bands at 1 THz, 1.66 THz and 2.1THz. The spectra were baseline corrected (see inset for the1.0 THz band). Larger deviations of the 2.1 THz band data points from the fitted line is due to the low S/N ratio of the band.

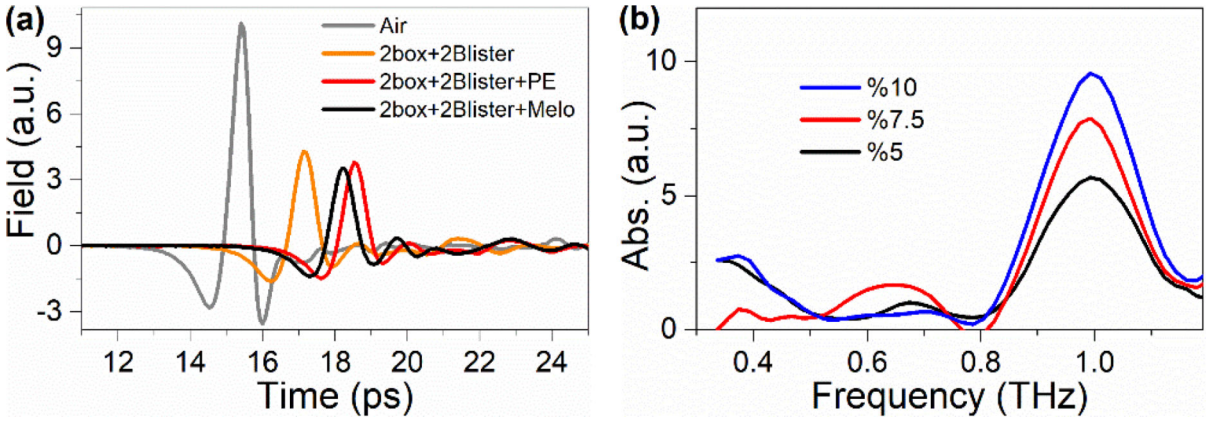

Fig. 6.

(a) Transmitted THz pulse profiles through drug host materials (box, plastic blister). (b) absorption spectrum of 5, 7.5 and 10 % Meloxicam in PE behind two box pieces and 2 blister samples to simulate the reflection sampling.

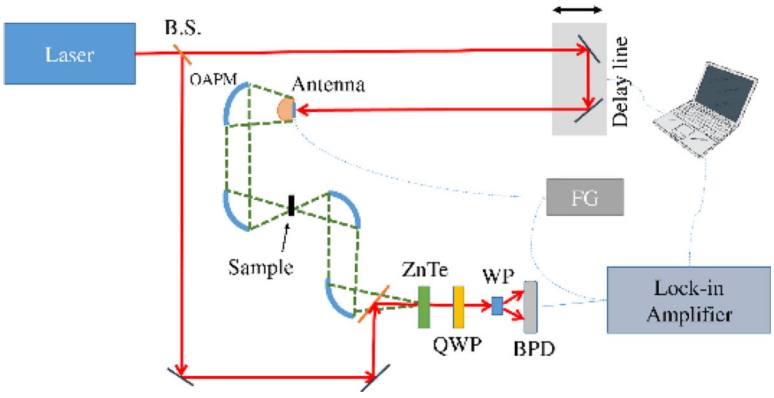

Scheme 1:
Terahertz time domain spectrometer optical setup.

Table 1

Frequencies of the vibrational modes observed in experimental and simulated spectra of Meloxicam.*

		Experimental (THz)		Solid State (THz)		Single Molecule (THz)			Description (SS-DFT frequency analysis)
	RT		77K	En. RT	En.	Cat.	An.	Zw.	
v1	1.00	strong, sharp	1.04	0.98	1.01	1.03	1.03	0.78	rotation along b axis
v_2	1.66	strong, sharp	1.70	1.64 1.75	1.67		1.81	1.67	rotation along c axis
v_3	2.07	strong, broad	2.08		2.12	2.04		1.97	wagging of the methyl group on the 5-membered ring of the molecule
v4	2.16	shoulder							
v_5	2.57	strong, sharp	(splitting) 2.33 2.61 2.93	2.57 2.68		2.43	2.4	2.53	torsional motion about the C-C bond connecting the two ring
v6	3.06	strong, sharp		3.01	2.94	3.05	2.70		skeletal motion resulting mainly displacement of CH_3 and H atoms of ring
v6	3.62	strong, sharp		3.64	3.44				out-of-plane torsion localized primarily at the sulfonyl group

*En: Enolic; Cat. Cationic; An. Anionic; Zw: Zwitter ionic, RT: Room Temp; SS-DFT: Solid State DFT